J. Chem. Thermodynamics 91 (2015) 459–473

Contents lists available at ScienceDirect

J. Chem. Thermodynamics

journal homepage: www.elsevier.com/locate/jct

Comprehensive study of the thermodynamic properties for 2-methyl-3-buten-2-ol

Dzmitry Zaitsau [a,b,*], Eugene Paulechka [c,d], Dzmitry S. Firaha [e], Andrey V. Blokhin [c], Gennady J. Kabo [c], Ala Bazyleva [d], Andrey G. Kabo [c], Mikhail A. Varfolomeev [b], Viktor M. Sevruk [c]

[a] Department of Physical Chemistry, University of Rostock, Dr-Lorenz-Weg 1, 18059 Rostock, Germany
[b] Department of Physical Chemistry, Kazan Federal University, Kremlevskaya str. 18, 420008 Kazan, Russia
[c] Chemistry Faculty, Belarusian State University, Leningradskaya 14, 220030 Minsk, Belarus
[d] Applied Chemicals and Materials Division, National Institute of Standards and Technology, Boulder, CO 80305-3337, USA
[e] Mulliken Center for Theoretical Chemistry, University of Bonn, Beringstr. 4+6, D-53115 Bonn, Germany

ARTICLE INFO

Article history:
Received 9 May 2015
Received in revised form 18 July 2015
Accepted 22 July 2015
Available online 29 July 2015

Keywords:
Heat capacity
Phase transition enthalpy
Vapour pressure
Hydrogen bond
Standard enthalpy of formation
Gas phase cluster formation

ABSTRACT

The heat capacity of 2-methyl-3-buten-2-ol over the interval $T = (5$ to $370)$ K was measured in an adiabatic calorimeter. The standard entropy and heat capacity of the liquid phase at a reference temperature 298.15 K were found to be $S^{o}_{m} = (232.6 \pm 1.0)\ J \cdot K^{-1} \cdot mol^{-1}$ and $C_{s,m} = (237.4 \pm 0.9)\ J \cdot K^{-1} \cdot mol^{-1}$. The triple-point temperature $T_{fus} = (245.03 \pm 0.03)$ K and the corresponding enthalpy of fusion $\Delta^{l}_{cr}H^{o}_{m} = (5.199 \pm 0.012)\ kJ \cdot mol^{-1}$ were also determined. The enthalpy of vaporisation was determined with a Calvet-type calorimeter to be $\Delta^{g}_{l}H^{o}_{m}(305.1\ K) = (46.9 \pm 1.6)\ kJ \cdot mol^{-1}$. The vapour pressure over the temperature interval (280 to 328) K was measured with a static technique. The standard entropy of vaporisation at $T = 298.15$ K was found to be $\Delta^{g}_{l}S^{o}_{m} = (132.7 \pm 0.2)\ J \cdot K^{-1} \cdot mol^{-1}$. The standard enthalpy of combustion for liquid 2-methyl-3-buten-2-ol $\Delta_{c}H^{o}_{m}(l,\ 298.15\ K) = -(3145.1 \pm 2.7)\ kJ \cdot mol^{-1}$ was measured with two static-bomb isoperibol combustion calorimeters. From the experimental data, the standard enthalpies of formation for liquid and gaseous 2-methyl-3-buten-2-ol were found to be $\Delta_{f}H^{o}_{m}(l,\ 298.15\ K) = -(251.6 \pm 2.8)\ kJ \cdot mol^{-1}$ and $\Delta_{f}H^{o}_{m}(g,\ 298.15\ K) = -(203.3 \pm 2.8)\ kJ \cdot mol^{-1}$, respectively. The latter value was confirmed by high-level quantum chemical calculations. Molecular association in the gas phase and its effect on thermodynamic properties of the compound were discussed.

1. Introduction

2-Methyl-3-buten-2-ol ($C_5H_{10}O$, CASRN 115-18-4) is one of the volatile organic compounds that are important in atmospheric chemistry, especially as precursors of tropospheric ozone [1,2]. For example, this compound was shown to account for approximately 20% of local OH reactivity in the Sierra Nevada Mountains in the day-time [3]. The main emitters of 2-methyl-3-buten-2-ol seem to be pine species [4]. Though only a limited number of plant species investigated emit 2-methyl-3-buten-2-ol, its emission may play an important role in regional photochemistry and could contribute a significant amount of acetone to the atmosphere [5]. On the other hand, this natural unsaturated alcohol, which is intensively emitted by pine needles, is one of two principal aggregation pheromone components of a spruce bark beetle, *Ips typographus*, aiding identification of sick trees by the beetle [6]. 2-Methyl-3-buten-2-ol is used mainly as a starting material or intermediate in the synthesis of medical drugs, vitamins A and E, and perfumes [7].

Available thermodynamic properties for the compound are limited to the vapour pressure [7–14], liquid heat capacity [7,8], and enthalpy of formation [15]. As demonstrated below, the available vapour–pressure data are inconsistent. In addition, such a flexible molecule with an –OH group is of intrinsic interest due to the possible mutual effects of rotating tops and hydrogen bonding. The latter results in molecular association in both the liquid and gas phases.

In this work, we report results of an experimental study of the thermodynamic properties of 2-methyl-3-buten-2-ol, including heat capacity in the condensed phases, temperatures and enthalpies of phase transitions, and enthalpies of combustion and formation in the liquid and gaseous states. Quantum chemical and statistical thermodynamic calculations are used to verify the gas-phase thermodynamic functions and to assess the effect of the molecular association on the reported properties.

* Corresponding author at: Department of Physical Chemistry, University of Rostock, Dr-Lorenz-Weg. 1, 18059 Rostock, Germany. Tel.: +49 177 5632394.
E-mail address: Zaitsaudz@gmail.com (D. Zaitsau).

http://dx.doi.org/10.1016/j.jct.2015.07.028
0021-9614/

2. Experimental

2.1. Sample

A commercial sample of 2-methyl-3-buten-2-ol (Sigma–Aldrich #136816) was dried over anhydrous $CuSO_4$ and distilled. The mole-fraction purity of the sample was 0.991 based on a fractional-melting study in an adiabatic calorimeter (table 1, figure 1). The mass fraction of the sample was determined to be 0.995 with a CHROM-5 chromatograph equipped with a thermal-conductivity detector. A SUPELCOWAX 10 capillary column of a 60 m length, 0.53 mm inner diameter, and 0.5 μm film thickness was used. The temperature of the column during the analysis was programmed to rise from t = (160 to 240) °C. The injector and detector temperatures were kept at 300 °C. This sample was used for measurement of the heat capacity, enthalpy of formation, and enthalpy of vaporisation.

A second commercial sample of 2-methyl-3-buten-2-ol (Alfa #B20790) was dried over anhydrous $CuSO_4$. No further purification was carried out. The degree of sample purity was determined with a gas chromatograph (GC) with a flame ionisation detector. A capillary column HP-5 was used with a 30 m length, 0.32 mm inner diameter, and 0.25 mm film thickness. The temperature of the column during the analysis was programmed to be t = 160 °C. Injector and detector temperatures were kept at 250 °C. The mass fraction of the primary component was found to be 0.998. The residual water content, 642 ppm, was determined by Karl Fischer titration. A Mettler DL35 Karl Fischer Titrator with Hydranal Composite 2 and Hydranal Eichstandard 5.0 (Riedel-de Haen) was used for the analysis. This sample was used for vapour–pressure determination. Descriptions of both samples used in this research are summarized in table 1.

2.2. Adiabatic calorimetry

The heat capacity of 2-methyl-3-buten-2-ol under vapour–saturation pressure (C_s) in the interval of (5 to 370) K and the properties of fusion were determined in a Termis TAU-10 adiabatic calorimeter. The apparatus and experimental procedures were described previously [16]. The sample was loaded into a calorimetric container of 1.13 cm^3 internal volume in a dry box to avoid moisture absorption. Depending on temperature, the heat capacity of the sample contributed (0.40 to 0.65) of the total heat capacity of the system. The equilibration times were close to 100 s at the lowest temperatures. At higher temperatures the equilibration times did not exceed 300 s for the crystal and 400 s for the liquid. In the pre-melting range, the equilibration took up to 4100 s.

The expanded uncertainty of the heat-capacity measurements was $4 \times 10^{-3} C_p$ in the interval of T = (20 to 370) K and gradually increased at lower temperatures, but did not exceed $2 \times 10^{-2} C_p$ at T = 5 K [16]. All the reported uncertainties correspond to the 0.95 confidence level for normal distribution ($k \approx 2$), unless stated otherwise.

In this experiment, two-phase (liquid + gas) heat capacities were determined and subsequently converted to C_s values using the methods described elsewhere [17]. Vapour pressures required for the conversion were obtained in this work, and recommended liquid-density values were taken from the NIST/TRC database [18].

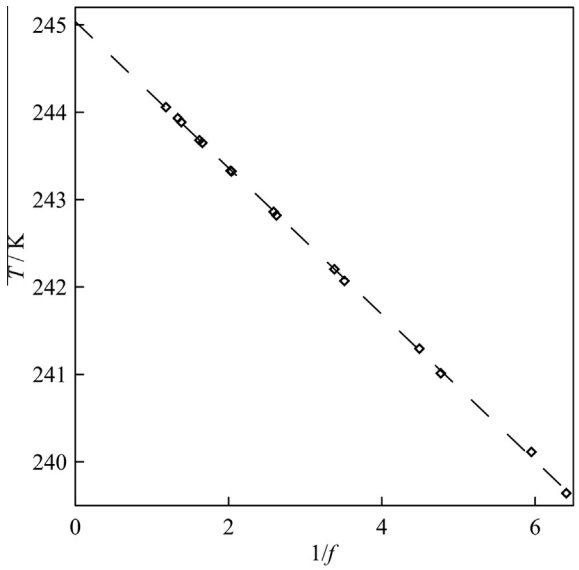

FIGURE 1. Results of the fractional-melting experiments for 2-methyl-3-buten-2-ol.

2.3. Vapour–pressure determination by static technique

2-Methyl-3-buten-2-ol has a vapour pressure near 3 kPa at T = 298.15 K. A static apparatus was used for measurement of the saturated vapour pressure over the liquid compound. The detailed description of the apparatus, procedures, uncertainty analysis, and a test with double-distilled water is given in the Supporting Information (table S1). Results of tests for this apparatus with benzoic acid, naphthalene, benzophenone, and ferrocene can be found elsewhere [19].

Briefly, the experimental setup consisted of a cylindrical cell made of 316Ti stainless steel with an internal volume of 20 cm^3. The cell was tightly connected to a tubing system with a VCR8 connector. The measuring cell was embedded in an aluminium heating block, whose temperature was kept constant within ±0.02 K. The uncertainty of the temperature determination was 0.05 K over the working temperature range of the system of (253 to 463) K. The temperature of the tubing connections between the measuring cell and pressure gauges was kept higher than those of the sample cell (by (30 to 50) K for liquid samples) to avoid condensation of sample. For this purpose, we used an air circulation thermostat with a temperature stability of ±0.2 K. The stainless-steel tube connected the sample cell with high-temperature capacitance manometers (MKS Instruments, Inc.) with the working range (0.1 to 10^5) Pa with a standard uncertainty of $5 \times 10^{-3} p$ as stated by the manufacturer.

TABLE 1
Materials used in the study.

Material	CASRN	Origin	Purification method	Purity (mass/mole fraction)	Method of analysis
2-Methyl-3-buten-2-ol	115-18-4	Sigma–Aldrich #136816	Distillation over $CuSO_4$	0.995 (mass) 0.991 (mole)	GC Fractional melting
2-Methyl-3-buten-2-ol	115-18-4	Alfa #B20790	Drying over CuSO4	0.998 (mass) 642 ppm water	GC Karl Fischer titration
Benzoic acid	65-85-0	VNIIFTRI	None	0.99993 (mass), K-2 grade	Certified
n-Undecane	1120-21-4	Reakhim	None	0.999 (mass)	GC
Naphthalene	91-20-3	Reakhim	None	0.999 (mass)	GC
Polyethylene	9002-88-4	Polimiz	Washing with acetone, vacuum drying	>0.99 (mass)	Elemental analysis

The reliability of the experimental setup and measuring technique was tested through measurement of the vapour pressure of water [20]. The measured values demonstrated that the expanded uncertainty (with 0.95 confidence level) in the pressure measurements is adequately described by the following expressions:

$$U(p/\mathrm{Pa}) = 0.1 + 0.01(p/\mathrm{Pa}) \text{ for } p_s < 1200 \text{ Pa}, \quad (1)$$

$$U(p/\mathrm{Pa}) = 10 + 0.01(p/\mathrm{Pa}) \text{ for } p_s > 1200 \text{ Pa}. \quad (2)$$

Before starting measurements, the empty measuring cell was connected to the system and evacuated to a pressure of 10^{-5} Pa with an Agilent HS-2 diffusion pump combined with an Agilent DS 202 rotary vane pump. Then, the static apparatus was disconnected from the evacuation line. If any pressure increase due to residual desorption from the tubing was detected, the heating and evacuation of the metal tubing were continued at a higher temperature. Finally, it was baked at the maximum temperature of 473 K until no pressure increase was observed.

To ensure complete degassing and removal of any solvent or moisture residue, the first few experiments at each temperature were used as *in situ* degassing and purification of the sample. If three to five consecutive measurement-degassing sequences at a selected temperature did not reveal systematic changes in the measured pressure, the sample was considered to be sufficiently degassed, and the measured value was assigned to the sample's saturation vapour pressure.

In a typical experimental cycle, a sample was placed inside the thermostatted measuring cell and connected to the measuring system. The cycle began with disconnecting the system from the vacuum pump and opening the valve between the sample cell and the pressure gauge. The pressure above the sample was monitored until stable values were obtained. After the measurement had been completed, the sample cell was disconnected from the pressure gauge by closing the valve, and the system was again evacuated. At least three consecutive vapour–pressure determinations were performed at each temperature with subsequent averaging of the results.

2.4. Vaporisation Calorimetry

For the direct determination of the enthalpy of vaporisation of 2-methyl-3-buten-2-ol, a differential Calvet-type microcalorimeter MID-200 equipped with modified cells was used [21]. The complete experimental procedure is described elsewhere [21]. A sample was placed into a hermetic cell made of stainless steel and covered with a thin nickel foil. After preliminary thermostatting of the cell, the foil was punctured with a rod, and thermal flow caused by evapouration of the sample was recorded. The calorimeter was calibrated with naphthalene and *n*-undecane using recommended values of the enthalpy of sublimation and vaporisation, respectively [22].

The enthalpy of vaporisation was obtained with the following equation:

$$\Delta_l^g H_m^o = M \int_0^\tau \frac{\Delta E}{K \cdot m} \mathrm{d}\tau \quad (3)$$

where m is the mass of the sample corrected for buoyancy; K is the calorimetric constant of the cell; ΔE is the difference of the thermocouple potentials, which corresponds to the temperature imbalance between the cell and the thermostat of the calorimeter at the time τ; and M is the molar mass of 2-methyl-3-buten-2-ol.

2.5. Combustion calorimetry

The energy of combustion of the liquid was measured in a modified commercial combustion calorimeter V-08 M with an isothermal water bath and a static bomb of 326 cm^3 volume (Calorimeter 1)[23] and in a calorimeter constructed in this laboratory with an isothermal air bath and a static bomb of 95.6 cm^3 volume (Calorimeter 2). Construction details and measurement procedures for Calorimeter 2 have been published [23,24]. The calibration of the calorimeters was carried out with reference benzoic acid (K-2 grade, mass-fraction purity of 0.99993).

The sample mass for each combustion experiment was determined with a Mettler Toledo AG 245 electronic balance with a repeatability of 2×10^{-5} g. Liquid samples were sealed in bags made of polyethylene film of 80 μm thickness and burned in a platinum crucible in an oxygen atmosphere of (3.11 ± 0.01) MPa at T = 298.15 K. Water of 1 cm^3 volume was added to the bomb before an experiment. After combustion, the liquid bomb content was titrated with 0.1 mol · dm^{-3} NaOH aqueous solution to determine the amount of nitric acid formed. The combustion products were checked for indications of incomplete burning (*i.e.*, traces of soot), and the mass of soot formed did not exceed 0.08 mg.

All calculations, including adjustment to standard state conditions and correction for incomplete burning, were performed by the methods described by Hubbard et al. [25]. The correction for nitric acid formation was based on the value −59.7 kJ · mol^{-1} for the molar energy of formation of 0.1 mol · dm^{-3} aqueous HNO_3 from the elements and H_2O (l) [26].

Based on the most recent assessment of the atomic masses, the molar mass of 2-methyl-3-buten-2-ol is in the range (86.125 to 86.139) g · mol^{-1} [27]. We have taken the middle of this range, 86.132 g · mol^{-1}, to be the molar mass of 2-methyl-3-buten-2-ol. The maximum uncertainty introduced to the molar enthalpy of formation by this assumption does not exceed 0.26 kJ · mol^{-1} and can be neglected, due to the larger experimental uncertainty. The enthalpy of formation of the compound was calculated using recommended enthalpies of formation of gaseous carbon dioxide, $\Delta_f H^\circ_m(CO_2, g) = -(393.51 \pm 0.13)$ kJ · mol^{-1}, and liquid water, $\Delta_f H^\circ_m(H_2O, l) = -(285.830 \pm 0.040)$ kJ · mol^{-1} [28].

IR spectra for liquid films of 2-methyl-3-buten-2-ol before and after the vapour–pressure determination were recorded with a Nicolet 380 FT-IR spectrometer equipped with a DTGS temperature-stabilized coated detector (4000 to 400) cm^{-1} at 4 cm^{-1} resolution and collection of 64 spectra. The detector was equipped with an attenuated total reflection (ATR) diamond crystal accessory.

2.6. Computational details

Computational aspects of this work include statistical thermodynamic evaluations of heat capacities and derived thermodynamic functions for the ideal gas, calculation of the enthalpy of formation for the ideal gas, and analysis of gas-phase association for the compound studied. All of these use the results of quantum-chemistry calculations as inputs. However, because various properties are required for each procedure, the calculations are performed at different levels of theory. The statistical thermodynamic calculations require frequencies of normal vibrations, and estimates of the molecular geometry and relative energies of the conformers. For calculation of the enthalpy of formation, total energies are most important. The quantitative description of molecular association is the most computationally demanding procedure, as it requires both high-level total energies and reliable frequencies of normal vibrations for, at least, the most stable conformers of oligomers, as well as estimates of molecular geometries and relative energies for a large number of conformers. Computation times were a necessary consideration.

Geometry optimization and calculation of frequencies of normal vibrations for the most stable conformers of the species studied were performed at the B3LYP/6-31+G* level of theory [29,30] with the Gaussian 09 package [31]. The relaxed potential-energy surface

scans for the rotating tops in the 2-methyl-3-buten-2-ol monomer were performed at the same level of theory with a systematic 5 degree change of the dihedral angles.

The number of possible structures for the trimer and tetramer of 2-methyl-3-buten-2-ol is very large. To speed up the calculations, we performed a search for possible structures of oligomers at the RI-BLYP-D3(BJ)/def2-SVP [30,32] level of theory with the ORCA package [33]. The resolution of identity (RI) approximation makes the time spent for evaluation of the most time-consuming exchange–correlation integrals proportional to N^2, where N is the number of basis functions, thus significantly reducing the computational time. In order to avoid the deficiency of the small basis set (def2-SVP), which is comparable with 6-31G*, the empirical geometry counterpoise (gCP) [34] correction coupled with the dispersion correction D3(BJ) from Grimme was introduced [35,36]. The relative energies obtained in this way were used to find the contribution of conformer mixing to the ideal-gas thermodynamic functions of oligomers, which was required for consideration of equilibria in molecular association.

If one is to calculate the energy change in a chemical reaction or in the process of molecular association with an uncertainty comparable to that of the experimental values, the total energies of the participating species need to be known as accurately as possible. Today, CCSD(T) is considered as the "gold standard" for this purpose [37]. However, the CCSD(T) approach scales dramatically with the number of basis functions ($\sim N^7$) and is too computationally expensive for large molecules or clusters. The recently proposed DLPNO-CCSD(T) [38] method is an alternative to CCSD(T) and is similarly accurate, while being affordable with respect to computational resources.

The "reference" total energies for the most stable conformers were obtained with the DLPNO-CCSD(T) method. Additionally, the RI-SCS-MP2 method [39], and two DFT methods, B3LYP and PW6B95, with the empirical dispersion correction D3(BJ) from Grimme et al. [35,36] were tested by comparison with the "reference" calculations. The SCS-MP2 method was chosen because it provided better thermochemistry than the conventional MP2 [40].

The results obtained were extrapolated to the complete basis set (CBS) following two-point procedures. For the Hartree–Fock and DFT calculations, the exponential extrapolation was applied [41], whereas for the RI-SCS-MP2 correlation energies, a power law was used [41]. The corresponding energies were taken from the single-point calculations X/def2-TZVPP//B3LYP/6-31+G* and X/def2-QZVPP//B3LYP/6-31+G*, where X is the method used. The applied basis sets were described elsewhere [42–44].

For the DLPNO-CCSD(T) calculations, extrapolation to the CBS was performed according to Hansen et al. [45], who assumed that the DLPNO-CCSD(T) and MP2 correlation energies have similar asymptotic behaviour, and the obtained total energies were denoted as DLPNO-CCSD(T)/δCBS//B3LYP/6-31+G*. A tight cut-off criterion (10^{-5} Hartree) was applied for calculations of the pair correlation energy.

The enthalpy of formation of the compound studied was calculated with the use of the methods listed above and the G4 method [46].

3. Results and discussion

3.1. Heat capacity

The experimental heat capacities for 2-methyl-3-buten-2-ol in the interval of $T = (5 \text{ to } 370)$ K are listed in table S2 and are shown in figure 2. The temperature dependence of the heat capacity for the liquid has a hump typical for alcohols (see, for example, Miltenburg et al. [47]).

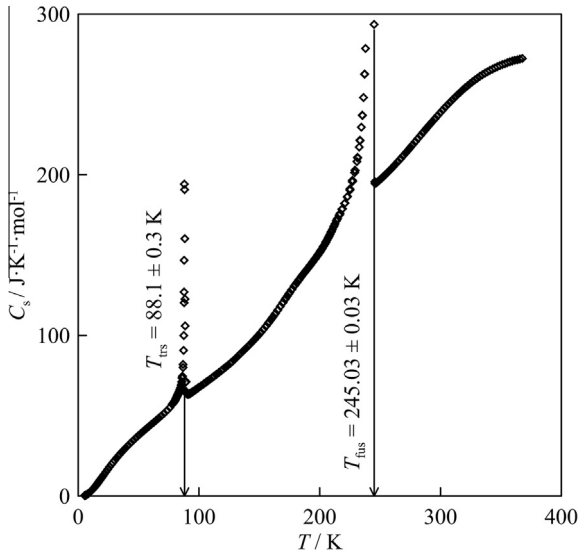

FIGURE 2. The temperature dependence of heat capacity for 2-methyl-3-buten-2-ol. Vertical lines indicate the phase transition temperatures.

The measured two-phase heat capacity C_{II} may differ significantly from the heat capacity under vapour saturation C_s. To assess the quality of our adjustment of C_{II} to C_s, an additional series of measurements were carried out for a small load of the studied liquid. The values of C_s were derived for both the series, and while the C_{II} values obtained in the two series differed by up to $0.04C_{II}$ (figure 3), the C_s values agreed within the uncertainty of the measurements.

Figures 4 and 5 summarize the data by Baglai et al. obtained in a differential adiabatic-type calorimeter with an uncertainty of about $0.02C_s$ [7,8], and the results of heat-capacity predictive schemes by Zábranský and Ruzicka [48] and by Kolska et al. [49]. The experimental heat capacities agree within their uncertainties. Neither of the predictive schemes can predict the C_s temperature dependence; however, the absolute values of heat capacity

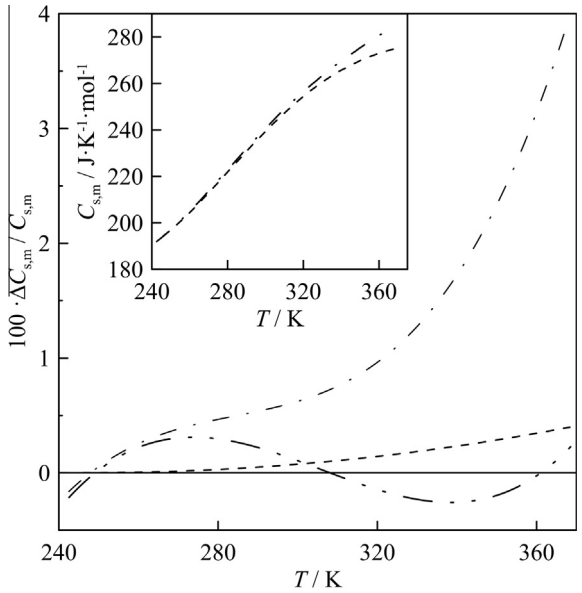

FIGURE 3. The effect of vaporisation of liquid 2-methyl-3-buten-2-ol during heat-capacity determination. ————, C_s determined with a large sample (≈0.6 g) and used as a reference for comparison; - - -, C_{II} for a large sample, - · - · -, C_{II} for a small (≈0.2 g) sample, - · - · - ·, C_s for a small sample.

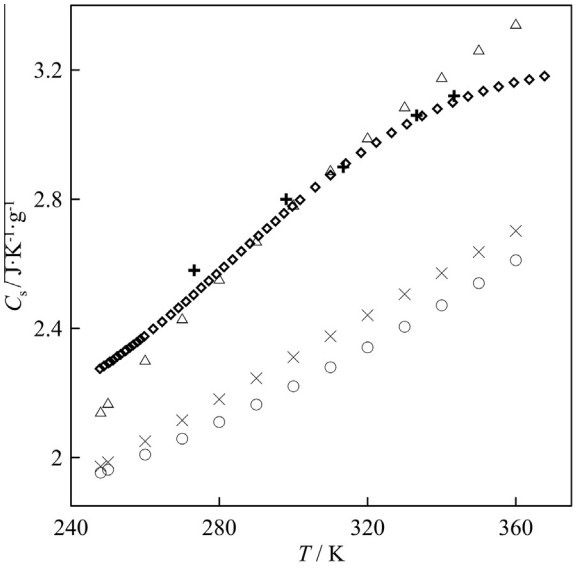

FIGURE 4. Comparison of the heat capacity for liquid 2-methyl-3-buten-2-ol; diamonds, this work; pluses, differential adiabatic CDA type calorimeter [7]; triangles, estimation according to the scheme of Zábranský and Růžička [48]; circles and ×, two estimation approaches by Kolska et al. [49].

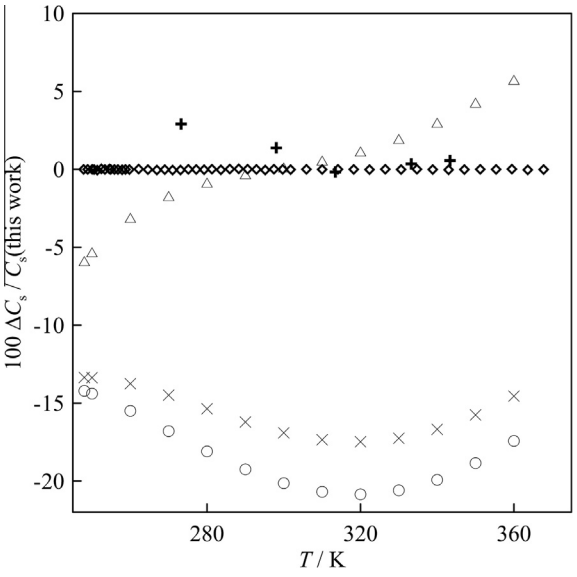

FIGURE 5. Deviation of the available heat capacity data for liquid 2-methyl-3-buten-2-ol from the results obtained in this work; diamonds, this work; pluses, differential adiabatic CDA type calorimeter [7]; triangles, estimation according to the scheme of Zábranský and Růžička [48]; circles and ×, two estimation approaches by Kolska et al. [49].

predicted according to Zábranský and Ruzicka [48] agree quite well with the experimental results. The poor predicting ability of group-contribution procedures for heat capacity of alcohols was noted recently by Straka et al. [50].

3.2. Low-temperature phase transition

An anomalous increase in the heat capacity of the sample was observed at temperatures below 100 K (figure 2). Phase transitions corresponding to structural changes or changes in mobility of molecules or atom groups occur usually at higher temperatures [51], while low-temperature transitions generally correspond to quantum effects. In the absence of any additional information, we considered the observed transition to be first-order. The thermodynamic parameters of the transition were determined from the results of four series of heat capacity experiments; T_{trs} = (88.1 ± 0.3) K, $\Delta_{trs}H^o_m$(88.1 K) = (170 ± 10) J · mol^{-1}, and $\Delta_{trs}S^o_m$(88.1 K) = (1.93 ± 0.11) J · K^{-1} · mol^{-1} (table 2). The transition temperature was determined as the maximum of heat capacity.

3.3. Fusion

Upon cooling the sample from T = 370 K, spontaneous crystallisation occurred at T = (240 to 243) K. The sample was kept at T = (243.2 to 243.3) K up to 6 h, until the heat evolution had stopped. Crystals obtained in this way were used in the measurements.

The triple-point temperature for 2-methyl-3-buten-2-ol T_{fus} = (245.03 ± 0.03) K was determined by the fractional melting method (figure 1). The corresponding enthalpy of fusion $\Delta^l_{cr}H^o_m$ = (5.199 ± 0.012) kJ · mol^{-1} was determined from four experiments (table 3). The following equation was used to calculate $\Delta^l_{cr}H^o_m$:

$$\Delta^l_{cr}H^o_m = Q - \int_{T_{start}}^{T_{fus}} C_{s,m}(cr)dT - \int_{T_{fus}}^{T_{end}} C_{s,m}(l)dT \quad (4)$$

where Q is the energy needed to heat 1 mol of 2-methyl-3-buten-2-ol from T_{start} to T_{end}. The initial T_{start} and final T_{end} temperatures lay in the temperature intervals with "normal" heat capacity for crystal and liquid, respectively.

The following equations were applied to describe the heat capacity for crystalline and liquid 2-methyl-3-buten-2-ol in equation (4):

$$C_{s,m}(cr)/J \cdot K^{-1} \cdot mol^{-1} = -44.769 + 0.98159\ (T/K), \quad (5)$$

$$C_{s,m}(l)/J \cdot K^{-1} \cdot mol^{-1} = 402.11 - 2.3156\ (T/K) + 5.9815 \cdot 10^{-3}\ (T/K)^2. \quad (6)$$

The numerical coefficients were obtained from the experimental data in the intervals of T = (169 to 190) K and (248 to 258) K, respectively.

3.4. Thermodynamic functions in the condensed state

Calculation of the absolute entropy of a compound is possible when the temperature dependence of the heat capacity is available from 0 K. The reported measurements cover the temperature range down to 5 K. Extrapolation of the heat capacity for the crystal from T = (5 to 0) K was performed with the use of the empirical function:

$$C_{s,m} = D_3(\theta_D/T) + E(\theta_E/T) \quad (7)$$

TABLE 2
Thermodynamic parameters of the crystal-to-crystal transition for 2-methyl-3-buten-2-ol.

$\frac{T_{start}}{K}$	$\frac{T_{end}}{K}$	$\frac{Q}{J \cdot mol^{-1}}$ [a]	$\frac{Q_1}{J \cdot mol^{-1}}$ [b]	$\frac{\Delta^{cr}_{cr}H^o_m}{J \cdot mol^{-1}}$
78.0	96.0	1273	1104	170
78.0	96.0	1276	1104	172
78.0	96.0	1279	1104	176
78.0	96.0	1265	1104	161
Average				170 ± 10[c]

[a] The total amount of heat introduced to the sample.
[b] The amount of heat used to heat up the crystal sample from T_{start} to T_{end}. One baseline for both phases was used: $C_{p,m}(cr)/J \cdot K^{-1} \cdot mol^{-1} = 48.008 - 0.15259\ (T/K) + 3.4989 \cdot 10^{-3}\ (T/K)^2$.
[c] The expanded uncertainty with 0.95 confidence level is applied.

TABLE 3
Determination of the molar enthalpy of fusion for 2-methyl-3-buten-2-ol.

T_{start}/K	T_{end}/K	Q/J · mol^{-1} [a]	$Q_{190-T_{start}}$/J · mol^{-1} [b]	Q_1/J · mol^{-1} [c]	Q_2/J · mol^{-1} [d]	$\Delta^{l}_{cr}H^{o}_{m}$/J · mol^{-1}
210.82	246.77	11,630	3190	9286	338	5196
208.80	246.83	11,970	2856	9286	350	5190 [e]
210.64	248.09	11,929	3160	9286	596	5207
210.30	245.52	11,480	3104	9286	95	5202 [e]
Average						5199 ± 12 [f]

[a] The total amount of heat introduced to the sample.
[b] The amount of heat needed to heat sample from T = 190 K (beginning of "melting region") to T_{start}.
[c] The amount of heat used to heat the crystal sample from T = 190 K to T_{fus} calculated using the heat-capacity baseline given by equation (5).
[d] The amount of heat used to heat the liquid sample from T_{fus} to T_{end} calculated using the heat-capacity baseline given by equation (6).
[e] From the fractional melting experiments.
[f] The expanded uncertainty with 0.95 level of confidence.

where $D_3(\theta_D/T)$ is the Debye heat-capacity function for three degrees of freedom, $E(\theta_E/T)$ is the Einstein heat-capacity function for one degree of freedom. From the experimental values of heat capacity over the temperature interval (5.4 to 6.7) K, the values of θ_D = 91.1 K and θ_E = 64.9 K for equation (7) were determined.

The experimental heat capacities in the interval T = (5 to 370) K were smoothed with polynomials. The derived thermodynamic functions for 2-methyl-3-buten-2-ol in the crystalline and liquid states are listed in table 4.

3.5. Vapour pressure and enthalpy of vaporisation

The experimental vapour pressures obtained in this work are listed in table 5. As the 2-methyl-3-buten-2-ol molecule has a double bond, the possibility of polymerization during vapour–pressure determination must be considered. IR spectra of the sample were recorded before and after the experiments (figure S3), and no significant difference was observed. As noted earlier, the difference in vapour pressure determined in the successive experiments did not exceed the uncertainty and had a random character. Additionally, after the vaporisation experiment, the sample was gently evaporated in a rotary evaporator at T = 293 K and a residual pressure of 100 Pa. The initial mass of the sample was (3.3867 ± 0.0010) g, and the residue after 1 h of such gentle vaporisation was (0.0034 ± 0.0014) g or (1.0 ± 0.4) · 10^{-3} of the initial sample mass. After subsequent 1 h vacuum treatment at T = 340 K, the mass of the non-volatile residue was (0.0015 ± 0.0015) g. This confirms no polymerization or other process resulted in formation of low-volatile compounds.

All the vapour pressure data available in the literature are shown in figures 6 and 7. The rigorous evaluation of the uncertainty of the experimental vapour pressures is not possible due to a lack of descriptions of the experimental techniques and parameters of experiments reported in the literature. Nevertheless, the estimated uncertainties are shown in figure S3 in Supporting Information. The vapour pressures obtained by a static method with a glass null manometer [7,8] are significantly higher than the results from this work. The static method with a glass null-manometer is very sensitive to the initial degassing and the purity of the studied sample. Once the sample is sealed in the glass manometer, *in situ* purification/degassing of the sample is not possible, and repeatability of vapour pressures obtained by this method does not mean that the sample is pure. Insufficient sample degassing increases the apparent vapour pressure and decreases the enthalpy of vaporisation evaluated from its temperature dependence.

The results by Zaretskii et al. [9] also deviate from the main trend of the experimental data. The vapour–pressure data reported by Roche [10] are available only as the Antoine equation $\log(P/\text{torr}) = 7.6091 - 1415.4/((t/°C) + 201.88)$, and the temperature interval studied is unknown. It is only reported that the lowest temperature of the interval is between (298 and 323) K.

Although most of these data refer to higher temperatures, the temperature intervals overlap with our measurements. Unfortunately, only parameters of the Antoine equation and its temperature interval are given in the works by Blazhin et al. [13] and by Pavlov et al. [14] and the temperature intervals do not overlap with our results.

The data by Raal and Brouckaert [11] and Lei et al. [12] are somewhat higher than the results obtained in this work. Their inclusion in the joint treatment of the experimental vapour pressures will result in a wrong slope of the ln p_s vs. T^{-1} dependence. Therefore, in further evaluations we used the experimental vapour pressures determined in the present work.

Numerical values of the weighted average of the enthalpy of vaporisation (see below) and heat capacity difference between the liquid and gas phases $\Delta_l^g C^o_{p,m}$ (298.15 K) = −104 J · K^{-1} · mol^{-1} were introduced into the Clarke–Glew equation [52] and the value of:

$$-R\Theta \ln(p_s(\Theta)/p^o) = (8786 \pm 5)\ \text{J} \cdot \text{mol}^{-1}\ (\Theta = 298.15\ \text{K}), \qquad (8)$$

was obtained. The repeatability of the experimental vapour pressures for 2-methyl-3-buten-2-ol was near 1%. This value corresponds to the uncertainty of the vapour–pressure determination by the static technique as given by equations (1) and (2).

3.6. Enthalpy of vaporisation

The results of calorimetric determination of the enthalpy of vaporisation at T = 305.12 K are given in table 6. The experimental value was adjusted to T = 298.15 K by using enthalpy increments for the liquid and gas phases ($\Delta^{298.15}_{305.12}\Delta_l^g H^o_m$ = 735 J · mol^{-1}). The resulting value is $\Delta_l^g H^o_m$(298.15 K) = (47.6 ± 1.6) kJ · mol^{-1}.

All enthalpies of vaporisation available in the literature are compared in table 7. The enthalpies of vaporisation were adjusted to T = 298.15 K with the enthalpy correction for the liquid and gas phases from adiabatic calorimetry and results of statistical calculations. The $RT^2(\text{d}\ln p_s/\text{d}T)$ value from the experimental vapour–pressure data corresponds to the $\Delta_l^g H_m/Z$ ratio, where Z is the compressibility factor [53]. The latter can be estimated as

$$Z = 1 + B_2 p_s/RT, \qquad (9)$$

where the second virial coefficient B_2 was evaluated using the Tsonopolous equation [54]. The estimated critical parameters needed for evaluation of the virial coefficient were taken from Yaws [55]. The second virial coefficient was found to be −2.26 dm^3 · mol^{-1} and the corresponding compressibility factor at T = 298.15 K was Z = 0.997. The final value of the enthalpy of vaporisation corrected for non-ideality was evaluated to be $\Delta_l^g H^o_m$

TABLE 4
Thermodynamic properties for 2-methyl-3-buten-2-ol in the condensed state (p^o = 0.1 MPa).[a]

T/K	$C_{s,m}$/J · K^{-1} · mol^{-1}	$\Delta_0^T H_m^o/T$/J · K^{-1} · mol^{-1}	S_m^o/J · K^{-1} · mol^{-1}	$-\Delta_0^T G_m^o/T$/J · K^{-1} · mol^{-1}
		Crystal II		
0	0	0	0	0
5	0.3244 ± 0.0065	0.0806 ± 0.0016	0.1073 ± 0.0021	0.0268 ± 0.0005
10	2.631 ± 0.026	0.677 ± 0.014	0.9010 ± 0.018	0.2245 ± 0.0045
15	6.921 ± 0.069	1.999 ± 0.025	2.701 ± 0.036	0.7016 ± 0.0090
20	12.04 ± 0.05	3.863 ± 0.042	5.385 ± 0.063	1.522 ± 0.017
25	17.22 ± 0.07	6.019 ± 0.045	8.631 ± 0.076	2.612 ± 0.021
30	22.12 ± 0.09	8.299 ± 0.051	12.21 ± 0.09	3.910 ± 0.026
35	26.55 ± 0.11	10.60 ± 0.06	15.96 ± 0.11	5.362 ± 0.032
40	30.53 ± 0.12	12.84 ± 0.06	19.77 ± 0.12	6.925 ± 0.039
45	34.27 ± 0.14	15.02 ± 0.07	23.58 ± 0.14	8.563 ± 0.045
50	37.80 ± 0.15	17.12 ± 0.08	27.38 ± 0.15	10.26 ± 0.05
60	44.33 ± 0.18	21.12 ± 0.09	34.85 ± 0.18	13.73 ± 0.07
70	50.70 ± 0.20	24.89 ± 0.11	42.16 ± 0.21	17.27 ± 0.08
80	57.08 ± 0.23	28.51 ± 0.12	49.35 ± 0.24	20.84 ± 0.09
88.1	62.25 ± 0.25	31.38 ± 0.13	55.10 ± 0.26	23.72 ± 0.11
		Crystal I		
88.1	61.32 ± 0.025	33.31 ± 0.14	57.03 ± 0.27	23.72 ± 0.11
90	62.35 ± 0.025	33.91 ± 0.14	58.35 ± 0.27	24.44 ± 0.11
100	67.72 ± 0.27	37.02 ± 0.15	65.19 ± 0.30	28.17 ± 0.12
110	73.25 ± 0.29	40.06 ± 0.17	71.91 ± 0.33	31.85 ± 0.14
120	78.98 ± 0.32	43.06 ± 0.18	78.52 ± 0.36	35.46 ± 0.15
130	85.52 ± 0.34	46.07 ± 0.19	85.10 ± 0.38	39.03 ± 0.17
140	92.84 ± 0.37	49.15 ± 0.20	91.70 ± 0.41	42.55 ± 0.18
150	100.8 ± 0.4	52.32 ± 0.21	98.37 ± 0.43	46.05 ± 0.20
160	110.3 ± 0.4	55.64 ± 0.23	105.2 ± 0.5	49.53 ± 0.21
170	121.0 ± 0.5	59.16 ± 0.24	112.2 ± 0.5	53.01 ± 0.22
180	131.9 ± 0.5	62.91 ± 0.25	119.4 ± 0.5	56.50 ± 0.24
190	141.7 ± 0.6	66.80 ± 0.27	126.8 ± 0.5	60.00 ± 0.25
200	151.5 ± 0.6	70.79 ± 0.29	134.3 ± 0.6	63.53 ± 0.27
210	161.4 ± 0.6	74.87 ± 0.30	141.9 ± 0.6	67.08 ± 0.28
220	171.2 ± 0.7	79.02 ± 0.32	149.7 ± 0.6	70.66 ± 0.29
230	181.0 ± 0.7	83.24 ± 0.34	157.5 ± 0.7	74.26 ± 0.31
240	190.8 ± 0.8	87.52 ± 0.35	165.4 ± 0.7	77.90 ± 0.32
245.03	195.7 ± 0.8	89.69 ± 0.36	169.4 ± 0.7	79.74 ± 0.33
		Liquid		
245.03	193.8 ± 0.8	110.9 ± 0.4	190.6 ± 0.8	79.74 ± 0.33
250	197.1 ± 0.8	112.6 ± 0.5	194.6 ± 0.8	81.98 ± 0.34
260	204.4 ± 0.8	116.0 ± 0.5	202.4 ± 0.9	86.46 ± 0.36
270	212.7 ± 0.9	119.4 ± 0.5	210.3 ± 0.9	90.90 ± 0.37
273.15	215.4 ± 0.9	120.5 ± 0.5	212.8 ± 0.9	92.29 ± 0.38
280	221.4 ± 0.9	122.9 ± 0.5	218.2 ± 0.9	95.31 ± 0.39
290	230.3 ± 0.9	126.4 ± 0.5	226.1 ± 0.9	99.70 ± 0.41
298.15	237.4 ± 0.9	129.4 ± 0.5	232.6 ± 1.0	103.2 ± 0.4
300	238.9 ± 1.0	130.0 ± 0.5	234.1 ± 1.0	104.0 ± 0.4
310	246.9 ± 1.0	133.7 ± 0.5	242.0 ± 1.0	108.4 ± 0.4
320	253.9 ± 1.0	137.3 ± 0.6	250.0 ± 1.0	112.7 ± 0.5
330	259.9 ± 1.0	141.0 ± 0.6	257.9 ± 1.1	116.9 ± 0.5
340	264.7 ± 1.1	144.5 ± 0.6	265.7 ± 1.1	121.2 ± 0.5
350	268.3 ± 1.1	148.0 ± 0.6	273.5 ± 1.1	125.4 ± 0.5
360	270.9 ± 1.1	151.4 ± 0.6	281.1 ± 1.2	129.7 ± 0.5
370	272.9 ± 1.1	154.7 ± 0.6	288.5 ± 1.2	133.8 ± 0.5

[a] Uncertainties reported in the table are the expanded uncertainty with 0.95 level of confidence. The expanded uncertainty for temperature is $U_c(T)$ = 0.01 K.

(298.15 K) = 48.5 · 0.997 = (48.35 ± 0.05) kJ · mol^{-1}. The enthalpy of vaporisation corrected for non-ideality agrees with the results of the calorimetric determination. By combining the evaluated enthalpy of vaporisation and vapour pressure at T = 298.15 K, one obtains the standard entropy of vaporisation $\Delta_l^g S_m^o$ (298.15 K) = $\Delta_l^g H_m^o$ (298.15 K)/298.15 K + $R\ln(p_s(298.15\ \mathrm{K})/(Z \times p^o))$ = 162.2 − 29.4 = (132.7 ± 0.2) J · K^{-1} · mol^{-1}.

3.7. Enthalpies of combustion and formation

The results of the determination of the energy of combustion for liquid 2-methyl-3-buten-2-ol are presented in table 8. The average standard molar energy and enthalpy of combustion at T = 298.15 K are as follows: $\Delta_c U_m^o(l)$ = −(3140.1 ± 2.7) kJ · mol^{-1} and $\Delta_c H_m^o(l)$ = −(3145.1 ± 2.7) kJ · mol^{-1}, where the uncertainty is the expanded uncertainty for the 0.95 confidence interval including repeatability, calibration uncertainty, and uncertainty of the combustion energy of benzoic acid and auxiliary compounds. The standard molar enthalpy of formation of the compound in the liquid state, $\Delta_f H_m^o(l)$ = −(251.6 ± 2.8) kJ · mol^{-1}, was calculated from the corresponding combustion reaction:

$$C_5H_{10}O\ (l) + 7O_2\ (g) = 5CO_2(g) + 5H_2O\ (l).$$

The experimental value deviates substantially from the enthalpy of formation reported by Gubareva et al. [15], $\Delta_f H_m^o(l, 298.15\ \mathrm{K})$ = −(177.9 ± 0.9) kJ · mol^{-1}. Gubareva et al. [15] used benzoic acid as an auxiliary material in the combustion of their samples. The combustion of benzoic acid caused the breaking of their glass ampules and combustion of the sealed material, but it

TABLE 5
Measured vapour pressures for 2-methyl-3-buten-2-ol.

T/K [a]	p_s/Pa [b]
Series 1	
322.89	12,514
325.36	14,315
320.59	11,107
315.80	8467
311.02	6405
306.13	4784
301.36	3534
295.88	2467
291.06	1787
286.31	1271
281.64	910.4
280.58	839.9
283.94	1075.5
288.63	1504
293.35	2084
298.84	2995
303.40	4006
308.18	5405
313.18	7252
313.25	7270
318.16	9605
322.94	12,476
325.39	14,242
320.62	11,021
315.81	8457
311.01	6393
306.16	4776
301.37	3532
295.92	2466
291.09	1780
285.82	1229.9
279.82	793.4
Series 2	
328.07	16,345
325.66	14,413
320.82	11,119
315.98	8484
279.12	747.7
280.94	860.8
283.31	1025.8
288.03	1447
293.17	2061
298.02	2863
303.03	3938
307.86	5284
312.70	7049

[a] The stability of the temperature was better than 0.02 K, the standard uncertainty of the temperature determination is $u(T) = 0.05$ K. The experimental points are listed in the order of determination.
[b] The standard uncertainty of the pressure measurements is described by: $u(p/\text{Pa}) = 0.05 + 0.005(p/\text{Pa})$ for $p_s < 1200$ Pa and $u(p/\text{Pa}) = 5 + 0.005(p/\text{Pa})$ for $p_s > 1200$ Pa.

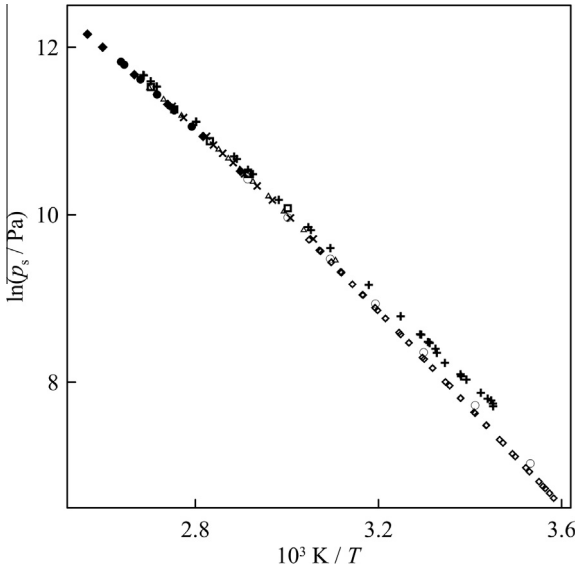

FIGURE 6. The temperature dependence of the vapour pressure for 2-methyl-3-buten-2-ol; diamonds, the results of static method determined in this work; pluses, the results of static method with a glass membrane as a null manometer by Baglai et al. [7,8]; squares, the results of Zaretskii *et al.* [9]; triangles, the ebulliometry data by Lei et al. [12]; ×, the ebulliometry data by Raal and Brouckaert [11]; open circles, the data from Roche Ltd. [10]; solid circles, the ebulliometry data by Blazhin et al. [13]; filled rhombs, data by Pavlov et al. [14].

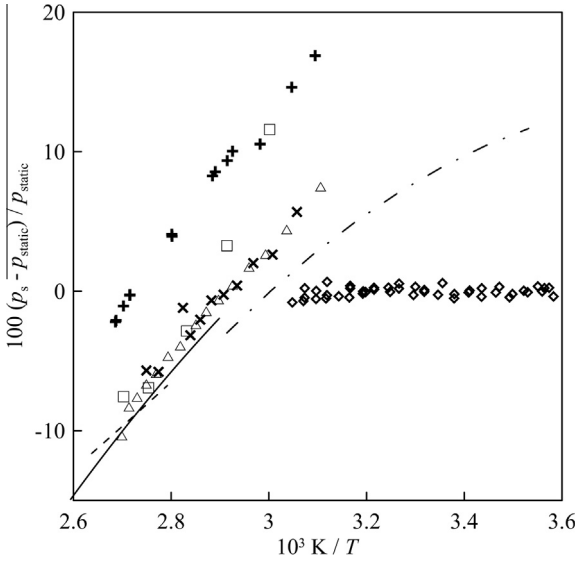

FIGURE 7. The deviation of the available vapour pressure data for 2-methyl-3-buten-2-ol from those measured in this work; diamonds, the results of static method determined in this work; pluses, the results of static method with a glass membrane as a null manometer by Baglai et al. (some data presented) [7,8]; squares, the results of Zaretskii et al. [9]; triangles, the ebulliometry data by Lei et al. [12]; ×, are the ebulliometry data by Raal and Brouckaert [11]; dash dot line (- · - · -), Antoine parameters from Roche Ltd [10]; dashed line (- - -), Antoine parameters Blazhin et al. [13]; solid line, Antoine parameters from data by Pavlov [14].

introduced additional errors because the energy of glass ampule cracking was not determined and considered in calculations. Also, no purity analysis of the sample used was provided.

The standard enthalpy of formation of 2-methyl-3-buten-2-ol in the gaseous state was derived in our research as the sum of the experimental enthalpies of vaporisation and formation in the liquid phase; $\Delta_f H^o_m(\text{g},298.15\text{ K}) = -(203.3 \pm 2.8)$ kJ · mol^{-1}.

We applied various empirical predictive procedures for estimation of the enthalpy of formation and the enthalpy of vaporisation of the compound studied. As one can see from the data listed in table 9, the best agreement of the experimental and predicted enthalpies of formation in the gas phase was obtained with the additive schemes by Cohen [56] and Pedley et al. [57]. In contrast, prediction of the enthalpy of vaporisation was less accurate in these cases. The best prediction of $\Delta^g_f H^o_m$, obtained with the "group contribution" scheme by Kolska et al. [58], deviates by 1.5 kJ · mol^{-1} from the experimental value. The deviations of the other schemes are much higher. The difference of 1.5 kJ · mol^{-1} is often acceptable for theoretical analysis, but this value corresponds to a 3% relative difference, whose effect on the thermal and mass analysis of industrial processes can be large.

TABLE 6
Results of calorimetric determination of the vaporisation enthalpy for 2-methyl-3-buten-2-ol.[a]

No.	$\frac{m}{g}$	$\frac{T}{K}$ [b]	$\int_{\tau=0}^{\tau} \Delta E \cdot d\tau$/mV · s [c]	$\frac{H}{J}$ [d]	$\Delta_l^g H_m^o$/kJ · mol^{-1}
1	0.16666	305.15	17,316	91.13	47.10
2	0.12893	304.95	13,140	69.16	46.20
3	0.25573	305.25	26,759	140.8	47.43
K = (190.0 ± 1.1) mV · s · J^{-1} [e]					
$\langle \Delta_l^g H_m^o$ (305.12 K)$\rangle$ = (46.9 ± 1.6) kJ · mol^{-1}					

[a] The expanded uncertainties for 0.95 confidence level are reported.
[b] The standard uncertainty of the temperature determination is $u(T)$ = 0.05 K.
[c] ΔE is the difference in the electric potential of the Peltier elements of the calorimeter.
[d] The enthalpy of vaporisation of the sample.
[e] K is the calibration constant converting the sum of electric potential into energy of the process under study.

TABLE 7
Enthalpies of vaporisation of 2-methyl-3-buten-2-ol determined in this work and reported in the literature.

T range/K	T_{av}/K	$\Delta_l^g H_m^o(T_{av})$[a]/kJ · mol^{-1}	$\Delta_l^g H_m^o$ (298 K)[a]/kJ · mol^{-1}	Method, reference
	305.12	46.9 ± 1.6	**47.6 ± 1.6**	Calorimetry, this work
280 to 325	303	47.98 ± 0.05	**48.51 ± 0.05** [b]	Static technique, this work
290 to 372	320	43.1 ± 0.2	45.5 ± 0.2	Static glass null manometer [7]
333 to 370	352	40.1 ± 1.4	46.0 ± 1.4	Ebulliometry [9]
N/A	N/A		46.8	N/A [10]
327 to 364	345.9	42.8 ± 0.6	**48.0 ± 0.7**[b]	Ebulliometry [11]
322 to 370	350	42.2 ± 0.4	**47.8 ± 0.5**[b]	Ebulliometry [12]
358 to 379	369	41.6	49.3	Ebulliometry [13]
345 to 390	369	40.6	48.3	Static[14]
The weighted average of selected $\Delta_l^g H_m^o$ (298 K) (in bold)			48.50 ± 0.05	
Value corrected for non-ideality of gas phase			48.35 ± 0.05	

[a] The enthalpy of vaporisation was adjusted to T = 298.15 K by using $\Delta_T^{298}H$(g) − $\Delta_T^{298}H$(l) values from adiabatic calorimetry and statistical calculations, the uncertainties in the corresponding enthalpy difference was introduced into the uncertainty of the final enthalpy of vaporisation.
[b] Experimental vapour pressures from the work in bold were chosen for joint treatment (see equation (8)).

3.8. Thermodynamic properties in the ideal-gas state

The methods of statistical thermodynamics were applied to calculate the thermodynamic properties in the ideal-gas state. The calculations were carried out in terms of the rigid rotor – harmonic oscillator – hindered-top rotation approximation.

As one can see from the optimised geometry of 2-methyl-3-buten-2-ol (figure 8), this molecule has four hindered rotors: two methyl, –OH and vinyl tops. The calculated frequencies of the normal modes corresponding to the internal rotation of these tops were as follows: 106 cm^{-1} for the vinyl top, 229 cm^{-1} and 260 cm^{-1} for the methyl tops, and 352 cm^{-1} for the –OH top. The parameters of internal rotation used for calculation of the gas-phase thermodynamic properties are listed in table 10. The reduced moments of inertia for the rotating tops were calculated according to Pitzer [59] from the optimised geometrical parameters of the most stable conformer of the molecule. The energy levels of internal rotation for each top were found by solving the Schrödinger equation for the hindered rotor (see Computational Details).

The symmetry number σ of the most stable conformer is equal to one, and the principal moments of inertia are (1.808×10^{-45}, 3.106×10^{-45}, and 3.062×10^{-45}) kg · m^2.

The calculated frequencies of normal modes systematically differ from the experimental vibrational frequencies [60]. The calculated values were scaled with frequency-dependent scaling factors to minimize this discrepancy. The vibrational spectrum of the studied compound was divided into three intervals. For each interval, a separate scaling factor $x = \omega_{exp}/\omega_{calc}$ was used. For the interval below 550 cm^{-1},

$$x = 1.0112 \pm 0.006, \quad (10)$$

was taken from our previous study of ethyl decanoate [61]. Where the numerical values of the scaling factors were estimated by the authors from the experimental and calculated frequencies of normal modes for ethane, propane, n-butane, n-pentane, n-hexane, iso-butane, 2,2-dimethylpropane, 2,2-dimethylbutane, and methyl acetate from an online database [60]. The same source was used for the scaling factor of C—H frequencies in the interval above 2700 cm^{-1},

$$x = 0.957. \quad (11)$$

For O—H stretching vibrations (3610 cm^{-1}) the value:

$$x = 0.978, \quad (12)$$

evaluated from the experimental and computed spectra of methanol in the gas phase was applied [62,63]. In the interval (550 to 2700) cm^{-1} the following equation was applied:

$$x = 1.005 - 2.6 \cdot 10^{-5}\omega_{calc}. \quad (13)$$

Only a few frequencies are not visible in the experimental vibrational spectra and, therefore, a possible error in the scaling factor will not have a significant effect on the final result.

The obtained values of thermodynamic properties in the ideal-gas state are reported in table 11. The calculated entropy of the 2-methyl-3-buten-2-ol at T = 298.15 K equal to 364.3 J · K^{-1} · mol^{-1} agrees very well with the value S_m^o (g, 298.15 K) = S_m^o (l, 298.15 K) + $\Delta_l^g S_m^o$ (298.15 K) = (365.2 ± 1.6) J · K^{-1} · mol^{-1} obtained from the experimental results.

The enthalpy of formation of 2-methyl-3-buten-2-ol in the ideal-gas state was calculated based on homodesmotic reactions:

TABLE 8
Results of determination of the standard molar energy of combustion for 2-methyl-3-buten-2-ol at $T = 298.15$ K.[a]

Property	Calorimeter 1		Calorimeter 2		
	1	2	3	4	5
$\frac{m_{comp}}{g}$	0.29792	0.27671	0.08706	0.14371	0.14123
$\frac{m_{fuse}}{g}$	0.00377	0.00309	0.00315	0.00272	0.00289
$\frac{m_{film}}{g}$	0.09019	0.08562	0.06114	0.06302	0.06724
$\frac{m_{soot}}{mg}$	0	0	0.03	0.08	0.01
$\frac{p(O_2)}{MPa}$	3.10	3.10	3.10	3.12	3.12
$\frac{T_{bath}}{K}$	302.15	302.15	301.65	301.65	301.65
$\frac{T_i}{K}$	24.90250	24.89481	25.06385	25.05085	25.04442
$\frac{T_f}{K}$	26.04177	25.96657	25.76478	25.96457	25.97204
$\frac{\Delta T_{corr}}{K}$	1.02604	0.95879	0.61617	0.83459	0.84553
$10^5 \frac{K}{s^{-1}}$	3.58	3.56	2.40	2.34	2.22
$\frac{\varepsilon_i}{J \cdot K^{-1}}$	14.98	14.91	7.39	7.56	7.57
$\frac{\varepsilon_f}{J \cdot K^{-1}}$	15.78	15.66	7.74	8.01	8.03
$\frac{\Delta_{ign}U}{J}$	0.17	0.4	0.12	0.22	0.31
$\frac{\varepsilon_{calor} \cdot (-\Delta T_{corr})}{J}$	−15097.05	−14107.54	−6054.49	−8200.68	−8308.18
$\frac{\varepsilon_{cont} \cdot (-\Delta T_{corr})}{J}$	−16.11	−14.94	−4.79	−6.71	−6.81
$\frac{\Delta_{IBP}U}{J}$	−15113.0	−14122.1	−6059.16	−8207.17	−8314.68
$\frac{m_{soot} \cdot \Delta_c U_{soot}}{J}$	0	0	−0.99	−2.64	−0.33
$\frac{\Delta U(HNO_3)}{J}$	3.58	1.73	2.27	3.34	2.75
$\frac{\Delta_{st.state}U}{J}$	4.47	4.12	2.61	3.74	3.79
$\frac{\Delta_c u^\circ}{J \cdot g^{-1}}$	−36470.4	−36499.1	−36424.4	−36454.0	−36439.1
$\frac{\Delta_c U^\circ_m}{kJ \cdot mol^{-1}}$	−3141.27	−3143.74	−3137.31	−3139.86	−3138.57

[a] m_{comp}, m_{fuse}, m_{film} are the masses of the sample of the studied compound, cotton fuse, and polyethylene bag adjusted to vacuum conditions (density of the compound is $\rho = 0.8205$ g · cm^{-3} [7], cotton fuse $\rho = 1.56$ g · cm^{-3}(data for glucose is used as reference) [67], polyethylene $\rho = 0.90$ g · cm^{-3} as stated by manufacturer); m_{soot} is the mass of the soot formed in the experiment; $p(O_2)$ is the pressure of oxygen in the bomb; T_{bath} is the temperature of the calorimeter; T_i and T_f it are the initial and final temperature in the reaction period; ΔT_{corr} is the corrected temperature rise; K is the cooling constant of the calorimeter; ε_i and ε_f are the energy equivalent of the contents of the bomb in the initial and final states, respectively; $\Delta_{ign}U$ is the electrical energy for igniting the sample; ε_{calor} is the energy equivalent of the calorimeter ($\varepsilon_{calor} = (14713.9 \pm 3.2)$ J · K^{-1} for calorimeter 1 and (9826.0 ± 2.5) J · K^{-1} for calorimeter 2, where the uncertainties are twice the standard deviation of the mean of 10 and 19 experiments); $\varepsilon_{cont} \cdot (-\Delta T_{corr}) = \varepsilon_i \cdot (T_i - 298.15) + \varepsilon_f \cdot (298.15 - T_i - \Delta T_{corr})$; $\Delta_c U_{soot}$ is the average combustion energy of the soot (−33 kJ · g^{-1}) [25]; $\Delta_{IBP}U$ is the change of internal energy for the isothermal bomb process; $\Delta U(HNO_3)$ is the energy required for decomposition of the HNO_3 solution formed; $\Delta_{st.state}U$ is the energy correction to the standard state (the sum of Washburn's corrections, for 2-methyl-3-buten-2-ol $c_p = 2.79$ J · K^{-1} · g^{-1}; $(\partial U/\partial p)_T = -0.46$ J · MPa^{-1} · g^{-1} [7]. For polyethylene $c_p = 2.53$ J · K^{-1} · g^{-1} [68], $(\partial U/\partial p)_T = -0.3$ J · MPa^{-1} · g^{-1}); $\Delta_c u^\circ$ and $\Delta_c U^\circ_m$ is the standard massic and molar combustion energies of 2-methyl-3-buten-2-ol, respectively. Value $\Delta_c u^\circ = -(46{,}299 \pm 31)$ J · g^{-1} for polyethylene was determined from 7 combustion experiments, $\Delta_c u^\circ = -(16945.2 \pm 16.8)$ J · g^{-1} for cotton thread was determined from 10 combustion experiments. In both cases twice the standard deviation is used as uncertainty.

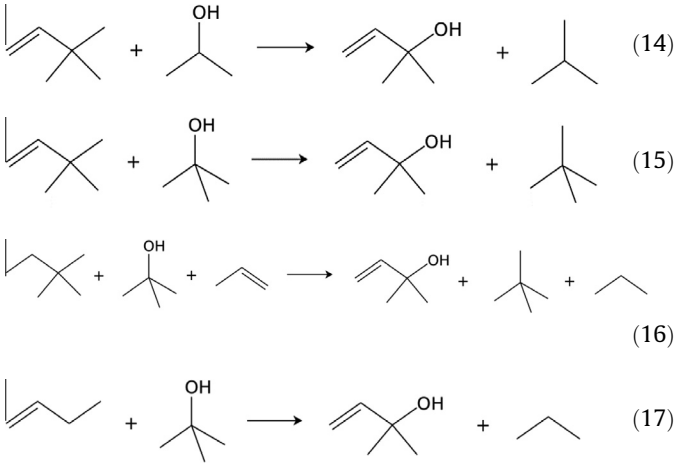

The enthalpy of these reactions can be expressed in two ways. The first method takes into account total energies E of all reaction participants, zero-point vibrational energies ZPVE, and thermal correction $\Delta_0^T H^\circ_m$:

$$\Delta_r H^\circ_m(T) = \left(\sum_{products} E - \sum_{reactants} E\right) + \left(\sum_{products} ZPVE - \sum_{reactants} ZPVE\right) + \left(\sum_{products} \Delta_0^T H^\circ_m - \sum_{reactants} \Delta_0^T H^\circ_m\right), \quad (18)$$

TABLE 9
Comparison of the enthalpies of formation in the liquid and gaseous phases at $T = 298.15$ K.

Method	$\Delta_f H^\circ_m$ (l)	$\Delta_f H^\circ_m$ (g)	$\Delta^g_f H^\circ_m$
	kJ · mol^{-1}	kJ · mol^{-1}	kJ · mol^{-1}
Experiment [this work]	−251.6	−203.3	48.35
Joback [69]		−182.1	45.0
Basařová [70]			51.3
Constantinou [71]	−222.1	−180.7	41.4
Ducros [72]			51.2
Verevkin [73]			53.1
Cohen [56]	−258.2	−207.4	50.8
Kolska [58]			49.6
Pedley [57]		−205.6	

where $T = 298.15$ K. In the second approach, the enthalpies of the reactions are derived from the enthalpies of formation of all the participants:

$$\Delta_r H^\circ_m(T) = \left(\sum_{products} \Delta_f H^\circ_m - \sum_{reactants} \Delta_f H^\circ_m.\right) \quad (19)$$

Since the left-hand sides of equations (18) and (19) are the same, corresponding transformations will allow calculation of the enthalpy of formation of a compound.

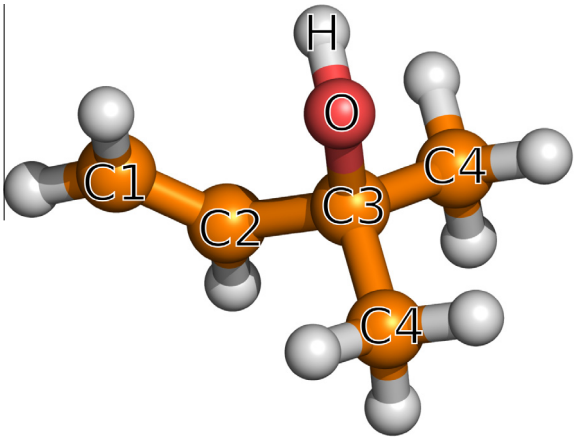

FIGURE 8. Equilibrium geometry of 2-methyl-3-buten-2-ol (C: orange; O: red, H: white). (For interpretation of the references to colour in this figure legend, the reader is referred to the web version of this article.)

We tested the performance of a number of levels of theory in the calculation of $\Delta_f H^\circ_m$ for the compound studied. As one can see (tables 12 and table S4), the best results were obtained with the DLPNO-CCSD(T)/CBS and G4 methods. The enthalpies of formation obtained from each reaction lie within the experimental uncertainty range.

3.9. Gas phase association and its effect on thermodynamic properties

The presence of the –OH group in 2-methyl-3-buten-2-ol is indicative of possible association in the gas phase. A bulky hydrocarbon substituent can either stabilize gas associates due to dispersion forces or destabilise them due to steric effects. To study the possibility of molecular association in the gas phase and evaluate the possible effect of this association on the thermodynamic properties, the following properties of the oligomers are required: equilibrium geometries of all conformers, their energies, and frequencies of normal vibrations.

In the molecule considered, internal rotation around C–O and C–C bonds is possible. In the oligomers, the possibility of different O···H–O–C3 dihedral orientations (figure 9) for the cyclic trimer and tetramer should be taken into account. Similar structures were previously computed for gas associates of methanol [64]. Linear forms of trimer and tetramer associates were found to be significantly less stable than the cyclic variants [64]. The cyclic forms with alternating values of O···H–O–C3 dihedrals were found to be more stable relative to systems with equal values.

Preliminary dimer, trimer, and tetramer structures were generated with random orientation of the substituents, whereas the structure between the hydrogen and oxygen atoms was kept similar to the methanol clusters. The randomly generated structures were optimised (see subsection Computational Details). Then, initial geometries for all the possible conformers were generated by

TABLE 10
Molecular parameters of 2-methyl-3-buten-2-ol used for statistical calculation of thermodynamic properties.

Top	Symmetry number σ	Reduced moment of inertia for rotating tops $10^{47} I_r$/kg · m^2	Potential function of internal rotation/kJ · mol^{-1}
$-CH_3$	3	5.17	$6.965\,(1-\cos(3\varphi))$
$-HC{=}CH_2$	1	18.8	$7.006 - 1.115\cos(\varphi) + 3.461\cos(2\varphi) + 4.342\cos(3\varphi) + 0.339\sin(3\varphi)$
–OH	1	1.44	$4.053 + 1.96\cos(2\varphi) + 3.17\cos(3\varphi)$

TABLE 11
Thermodynamic properties of 2-methyl-3-buten-2-ol monomer in the ideal gas state.

T/K	S°_m/J · K^{-1} · mol^{-1}	$C^\circ_{p,m}$/J · K^{-1} · mol^{-1}	$\Delta^T_0 H^\circ_m/T$/J · K^{-1} · mol^{-1}	$-\Delta^T_0 G^\circ_m/T$/J · K^{-1} · mol^{-1}	$\Delta_f H^\circ_m$/kJ · mol^{-1}	$\Delta_f G^\circ_m$/kJ · mol^{-1}
50	230.0	39.2	34.9	195.2	−181.0	−169.2
100	263.2	60.2	41.9	221.2	−187.7	−154.6
150	291.8	81.8	51.7	240.1	−192.2	−136.9
200	317.9	100.4	61.6	256.3	−196.2	−117.9
273.15	352.9	125.4	75.4	277.6	−201.6	−88.4
298.15[a]	**364.3**	**133.6**	**79.9**	**284.4**	**−203.3**	**−78.0**
300	365.1	134.2	80.3	284.8	−203.4	−77.2
400	408.0	164.5	97.6	310.3	−209.6	−34.1
500	447.5	190.2	113.7	333.9	−214.6	10.3
600	484.2	211.6	128.3	355.9	−218.6	55.7
700	518.2	229.7	141.5	376.7	−221.7	101.7
800	549.9	245.2	153.5	396.4	−223.9	148.3
900	579.6	258.7	164.5	415.1	−225.5	194.6
1000	607.5	270.4	174.5	433.0	−226.4	241.3

[a] The experimental S°_m (g, 298.15 K) = 365.2 ± 1.6 J · K^{-1} · mol^{-1}.

TABLE 12
The enthalpy of formation (kJ · mol^{-1}) in the gaseous state for 2-methyl-3-buten-2-ol at T = 298.15 K calculated at the levels of theory X//B3LYP/6-31+G*.

Reaction method	B3LYP/6-31+G*	DLPNO-CCSD(T)/CBS	RI-SCS-MP2/CBS	B3LYP-D3/CBS[a]	PW6B95-D3/CBS[a]	G4
(14)	−207.5	−204.2	−203.4	−204.8	−204.9	−205.0
(15)	−205.4	−204.5	−203.9	−204.6	−204.7	−205.1
(16)	−208.2	−205.1	−206.1	−205.4	−205.4	−205.1
(17)	−202.6	−203.1	−203.6	−203.6	−204.2	−203.3
Average	−205.9	−204.2	−204.3	−204.6	−204.8	−204.6
MAD[b]	4.9	1.8	2.8	2.1	2.1	1.8

[a] Total energies evaluated with DFT methods were extrapolated to complete basis set similar to the Hartee−Fock energies.
[b] Maximal absolute deviation from the experimental enthalpy of formation in the gas phase $\Delta_f H^\circ_m$ (298.15 K) = −203.3 kJ · mol^{-1}.

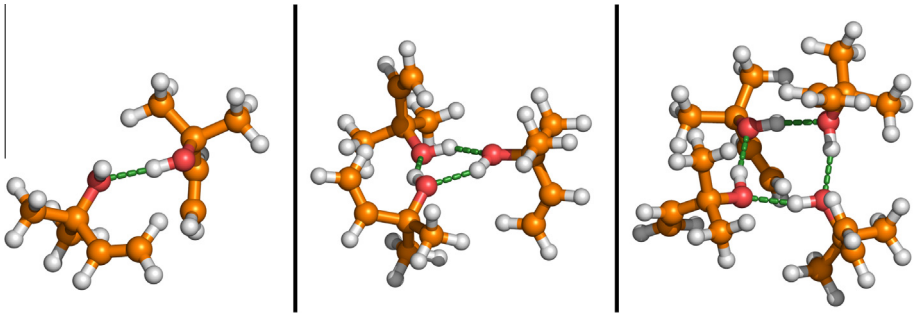

FIGURE 9. Equilibrium geometry of the dimer (left), the trimer (center), and the tetramer (right) of 2-methyl-3-buten-2-ol. Green dashed line represents the hydrogen bond between O and H. (For interpretation of the references to colour in this figure legend, the reader is referred to the web version of this article.)

combination of minima for C1–C2–C3–O (0°, 120° and 240°) and C2–C3–O–H (60°, 180° and 300°) dihedral angles and then optimised. Finally, duplicates obtained after optimization were removed.

In total, $3^4 = 81$ conformers were obtained for the dimer, and they all were confirmed by subsequent optimization. In the case of the trimer, the number of potential conformers $3^6 \cdot 2 = 1458$ is doubled because three O···H–O–C3 dihedrals can have the same sign (*e.g.*, **uuu** orientation) or one can differ from the other two (*e.g.*, **uud**), see figure 10. After optimization, the final set was checked to confirm the absence of geometry duplication with the help of the quaternion characteristic polynomial (QCP) method [65], and thus, the number of conformers was reduced to 1417.

For methanol clusters, the stable tetramer forms were **udud** and **uudd** [64]. The presence of a bulky hydrocarbon substituent in 2-methyl-3-buten-2-ol distorted the plane of the O–H and the hydrogen bonds in such way that the hypothetical **uuuu**, **uuud**, and **uudd** orientations converted into **udud**. The total number of potential **udud** conformers $3^8 = 6561$ was also analysed with the QCP method and was reduced to 6560 structures after optimization.

Each dimer, trimer, and tetramer conformer has an enantiomeric counterpart, which was also considered in calculation of the thermodynamic parameters for association in the gas phase.

In the calculations of thermodynamic properties of the association process, the products of the principal moments of inertia and frequencies of normal vibrations required for calculation of rotational and vibrational contributions were calculated for the most stable structures. The frequencies were scaled with equations (10)–(13). The relative energies of the conformers obtained at $T = 0$ K were used to determine the conformational mixing contribution for the considered species.

The energy differences between the oligomers at $T = 0$ K were calculated at the levels of theory considered above (except G4 method). The enthalpy differences at various temperatures (table 13) were determined with $H(T) - H(0)$ values obtained as described earlier and ZPVE calculated at the B3LYP/6-31+G* theory level and scaled according to equations (10)–(13). The contribution of the gas-phase association to the heat capacity of 2-methyl-3-buten-2-ol was evaluated numerically.

The results of statistical thermodynamic calculations (table 13) are reported at $T = 298.15$ K, the reference temperature for thermochemical investigations, and $T = 370$ K, near the normal boiling temperature of 2-methyl-3-buten-2-ol. At the temperatures considered and $P = 0.1$ MPa, the effect of oligomerization is small to negligible. At $T = 298.15$ K the maximum amount of oligomeric structures was found to be ~0.1% for the trimer structure (DLPNO-CCSD(T)/δCBS). At the same time, the error in the values of the standard Gibbs energies obtained is near $4\ \mathrm{kJ \cdot mol^{-1}}$, so the molar part of the trimer can increase to 1% as well as reduce to 0.001%. Therefore, the evaluation of the equilibrium concentrations should be carried out with care.

As one can see, the RI-SCS-MP2/CBS level of theory systematically underestimates the binding energy within the gas cluster, this underestimation increases with the size of the cluster. On the other hand, the B3LYP-D3(BJ)/CBS method overestimates the binding energy in the cluster. In the case of trimers and tetramers, the deviation from the DLPNO-CCSD(T)/δCBS method becomes too large even for qualitative analysis of gas-phase association. Interestingly, the PW6B95-D3(BJ)/CBS results allow determination of the energies of gas phase molecular clusters very close to the reference DLPNO-CCSD(T)/δCBS method, where even for large clusters, the energy difference was lower than $3\ \mathrm{kJ \cdot mol^{-1}}$. The results evaluated at the DLPNO-CCSD(T)/δCBS level of theory apparently show the absence of oligomerization either at the reference temperature 298.15 K or at 370 K (near the normal boiling temperature). Nonetheless, even a low content of oligimeric forms can contribute to the heat capacity of gas-phase values at levels

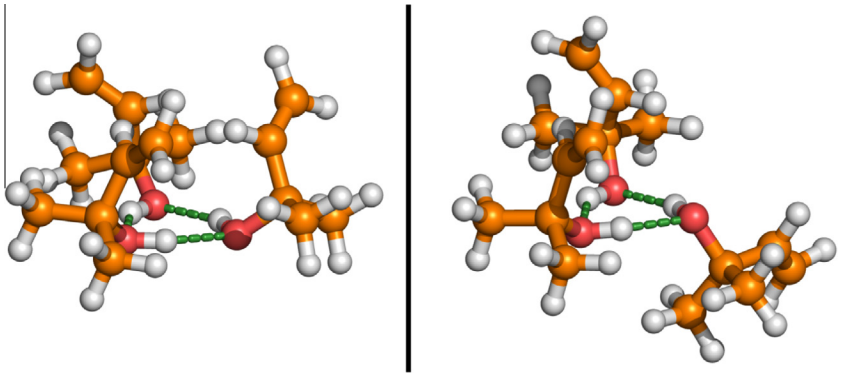

FIGURE 10. The trimer of 2-methyl-3-buten-2-ol in **uuu** (left) and **uud** (right) orientations.

TABLE 13
Thermodynamic parameters of association for 2-methyl-3-buten-2-ol.

X[a]	$\Delta_{bind}H^{o}_{m}$ [b]/kJ · mol^{-1}	$\Delta_{bind}S^{o}_{m}$ [b]/J · K^{-1} · mol^{-1}	$\Delta_{bind}G^{o}_{m}$ [b]/kJ · mol^{-1}	x[c](0.1 MPa)	$x\cdot\Delta_{bind}H^{o}_{m}$/J · mol^{-1}	$\Delta_{bind}C^{o}_{p,m}$ [d]/J · K^{-1} · mol^{-1}
			T = 298.15 K			
			Dimer			
DLPNO-CCSD(T)/δCBS	−18.7	−126.1	18.9	$4.9\cdot10^{-4}$	−9.1	0.3
PW6B95-D3/CBS	−18.4		19.2	$4.4\cdot10^{-4}$	−8.1	0.2
B3LYP-D3/CBS	−21.9		15.7	$1.8\cdot10^{-3}$	−39	1.3
RI-SCS-MP2/CBS	−17.8		19.8	$3.3\cdot10^{-4}$	−5.9	0.2
			Trimer			
DLPNO-CCSD(T)/δCBS	−57.2	−249.7	17.3	$9.4\cdot10^{-4}$	−53	4.4
PW6B95-D3/CBS	−57.9		16.6	$1.2\cdot10^{-3}$	−72	6.0
B3LYP-D3/CBS	−66.2		8.3	0.028	−1832	131
RI-SCS-MP2/CBS	−56.1		18.4	$6.0\cdot10^{-4}$	−34	2.7
			Tetramer			
DLPNO-CCSD(T)/δCBS	−103.0	−434.8	26.6	$2.2\cdot10^{-5}$	−2.2	0.3
PW6B95-D3/CBS	−105.6		24.1	$6.1\cdot10^{-5}$	−6.4	1.0
B3LYP-D3/CBS	−122.9		6.7	0.049	−5991	734
RI-SCS-MP2/CBS	−100.9		28.7	$9.2\cdot10^{-6}$	−0.9	0.1
			T = 370 K			
			Dimer			
DLPNO-CCSD(T)/δCBS	−17.6	−122.7	27.8	$1.2\cdot10^{-4}$	−2.1	0.04
PW6B95-D3/CBS	−17.3		28.1	$1.1\cdot10^{-4}$	−1.9	0.04
B3LYP-D3/CBS	−20.8		24.6	$1.3\cdot30^{-4}$	−6.9	0.15
RI-SCS-MP2/CBS	−16.6		28.8	$8.7\cdot10^{-5}$	−1.4	0.03
			Trimer			
DLPNO-CCSD(T)/δCBS	−55.9	−246.0	35.1	$1.1\cdot10^{-5}$	−0.6	0.03
PW6B95-D3/CBS	−57.3		33.8	$1.7\cdot10^{-5}$	−1.0	0.1
B3LYP-D3/CBS	−65.6		25.4	$2.6\cdot10^{-4}$	−17	1.0
RI-SCS-MP2/CBS	−55.4		35.6	$9.5\cdot10^{-6}$	−0.5	0.03
			Tetramer			
DLPNO-CCSD(T)/δCBS	−101.6	−430.6	57.7	$7.2\cdot10^{-9}$	$-7.3\cdot10^{-4}$	0.0
PW6B95-D3/CBS	−104.2		55.1	$1.6\cdot10^{-8}$	$-1.7\cdot10^{-3}$	0.0
B3LYP-D3/CBS	−121.5		37.8	$4.6\cdot10^{-6}$	$-5.6\cdot10^{-1}$	0.06
RI-SCS-MP2/CBS	−99.5		59.8	$3.6\cdot10^{-9}$	$-3.6\cdot10^{-4}$	0.0

[a] Calculations were performed at the X//B3LYP/6-31+G* levels of theory.
[b] Binding corresponds to the formation of oligomeric structures from monomers: *e.g.* 4 monomer = tetramer. $\Delta_{bind}H^{o}_{m}$, $\Delta_{bind}S^{o}_{m}$, and $\Delta_{bind}G^{o}_{m}$ are the enthalpy, entropy, and standard Gibbs energy change of the formation of corresponding oligomeric structure.
[c] The mole fraction of the oligometric structure in the gas phase.
[d] $\Delta_{bind}C^{o}_{p,m}$ corresponds to the change in the heat capacity of ideal gas due to gas phase assossiation.

comparable or higher than the evaluated uncertainty. Thus, the gas-phase heat capacity is more affected by the oligomerization than the standard entropy of the gas phase.

We have evaluated the temperature distribution of the gas-phase composition for 2-methyl-3-buten-2-ol at P = 0.1 MPa (see figure 11) for the suggested reference method (DLPNO-CCSD(T)/δCBS). As one can see, the size of the gas-phase clusters of 2-methyl-3-buten-2-ol is decreased with increasing temperature. From the main trend of the distribution presented, the dimer cluster, hypothetically, should be the most abundant structure at T = 298.15 K. However, the maximal content of dimer does not exceed 0.2 mol% of the gas-phase mixture. This fact is indirectly supported by the close agreement (within 1 J · K^{-1} · mol^{-1}) between the statistically calculated and experimental value of the standard entropy for the gas at T = 298.15 K shown earlier.

Changing the pressure from P = 0.1 MPa to p_s substantially changes the distribution of the oligomer structures in the gas phase. The results are presented in figure 12. The amount of tetramer, as well as trimer, is insignificant up to 600 K. The amount of dimer obtained is only 0.03% of the mixture at such high temperature.

In methanol, a tetramer is responsible for a significant deviation of the gas-phase heat capacity from the ideal value at pressures close to 0.1 MPa [66]. Calculations of the gas-phase tetramerization for methanol demonstrate that $\Delta_r H°$ at T = (298.15 to 370) K differs

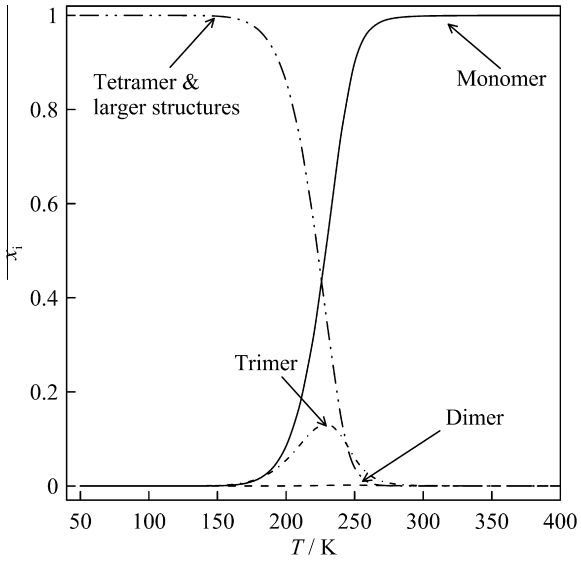

FIGURE 11. The temperature distribution of the gas phase composition for 2-methyl-3-buten-2-ol at standard conditions (P^o = 0.1 MPa) evaluated at DLPNO-CCSD(T)/δCBS level of theory: x_i is the molar composition of the gas phase; solid line, is the content of single molecule, dashed line, is the dimer cluster content, dash dot line, corresponds to the trimer structure content, dash dot dot line, shows the tetramer and higher size clusters content.

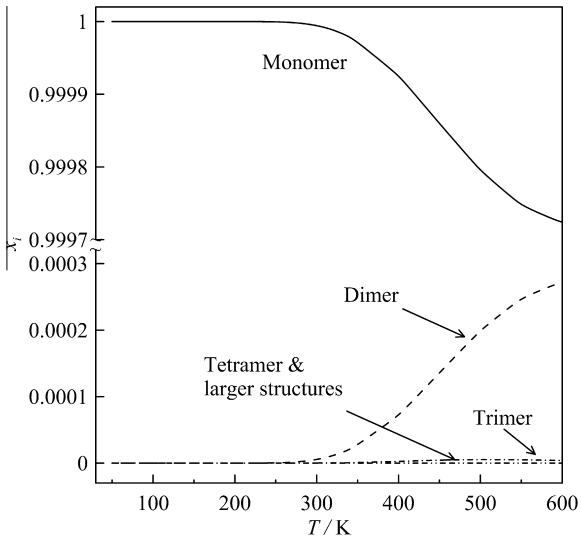

FIGURE 12. The temperature distribution of the gas phase composition for 2-methyl-3-buten-2-ol at saturated vapour–pressure conditions evaluated at DLPNO-CCSD(T)/δCBS level of theory: x_i is the molar composition of the gas phase; solid line, is the content of single molecule, dashed line, is the dimer cluster content, dash dot line, corresponds to the trimer structure content, dash dot dot line, shows the tetramer and higher size clusters content.

from that of 2-methyl-3-buten-2-ol by less than 2 $kJ \cdot mol^{-1}$. The entropy change $\Delta_r S°$ is about 60 $J \cdot K^{-1} \cdot mol^{-1}$ more negative for 2-methyl-3-buten-2-ol. The latter molecule has a larger mass and moments of inertia. As a result, the translational and rotational contributions to $\Delta_r S°$ are more negative and they cannot be compensated by the increased vibrational and conformational contributions. Therefore, the main reason for the reduced tendency of the gas-phase association for 2-methyl-3-buten-2-ol compared to methanol is the larger size of the molecule. In the liquid phase, $\Delta_r S°$ is much lower than in the gas phase, and the strong tendency to associate holds. This is evidenced by the hump observed in the temperature dependence of the liquid heat capacities.

4. Conclusions

The thermodynamic properties for 2-methyl-3-buten-2-ol were determined in the condensed and gaseous phases. The mutual consistency of the experimental values and the results of quantum chemical calculations indicates reliability in the values determined, as well as significant progress in computational methods towards prediction of the gas-phase enthalpy of formation. A comparison with values predicted by available group contribution schemes revealed that the scheme by Cohen [56] shows good predicting ability for the enthalpy of formation of the compound. Prediction of the enthalpy of vaporisation for branched and substituted alcohols is still a challenging problem.

The total energies form the DLPNO-CCSD(T)/δCBS method were used as a reference to study the association of the 2-methyl-3-buten-2-ol molecules in the gas phase. It was found that the contribution of the oligomerization process on the gas-phase thermodynamic properties for this compound is negligible at P = 0.1 MPa and T = (298 to 370) K.

Acknowledgements

Dr Zaitsau is grateful to the Russian Government Program of Competitive Growth of Kazan Federal University for financial support of this work.

Appendix A. Supplementary data

Supplementary data associated with this article can be found, in the online version, at http://dx.doi.org/10.1016/j.jct.2015.07.028.

References

[1] S.A. McKeen, E.-Y. Hsie, S.C. Liu, J. Geophys. Res. 96 (1991) 15377–15394.
[2] F. Fehsenfeld, J. Calvert, R. Fall, P. Goldan, A.B. Guenther, C.N. Hewitt, B. Lamb, S. Liu, M. Trainer, H. Westberg, P. Zimmerman, Global Biogeochem. Cycles 6 (1992) 389–430.
[3] M.S. Lamanna, A.H. Goldstein, J. Geophys. Res. 104 (1999) 21247–21262.
[4] P. Harley, V. Fridd-Stroud, J. Greenberg, A. Guenther, P. Vasconcellos, J. Geophys. Res. 103 (1998) 25479–25486.
[5] C. Ferronato, J.J. Orlando, G.S. Tyndall, J. Geophys. Res. 103 (1998) 25579–25586.
[6] B.S. Lanne, P. Ivarsson, P. Johnsson, G. Bergström, A.-B. Wassgren, Insect Biochem. 19 (1989) 163–167.
[7] A.K. Baglai, L.L. Gurarii, G.G. Kuleshov, J. Chem. Eng. Data 33 (1988) 512–518.
[8] A.K. Baglai, A.A. Baev, V.P. Belousov, V.V. Beregovykh, M.M. Grushenko, L.L. Gurarii, S.G. Konstantinov, Y.L. Kostyushko, G.G. Kuleshov, N.I. Pasechnik, R.I. Petrashkevich, A.I. Podkovyrov, A.A. Sitnov, M.A. Shishko, I.L. Shulgin, Khim. Farm. Zhur. 18 (1984) 1013–1019.
[9] M.I. Zaretskii, E.M. Chartov, L.A. Pushkina, V.V. Elkin, V.V. Rusak, Zh. Prikl. Khim. 72 (1999) 1436–1439 (S.-Peterburg).
[10] B. F. Hoffmann-La Roche Ltd, 1990. <http://www.inchem.org/documents/sids/sids/115184.pdf>.
[11] J.D. Raal, C.J. Brouckaert, Fluid Phase Equilib. 74 (1992) 253–270.
[12] Y. Lei, H. Li, L. Zhu, S. Han, Fluid Phase Equilib. 206 (2003) 87–94.
[13] Y.M. Blazhin, S.K. Ogorodnikov, A.I. Morozova, S.V. Kazakova, L.N. Volkova, Zh. Prikl. Khim. 47 (1974) 184–187.
[14] A.I. Pavlov, A.D. Peschenko, V.I. Zubkov, Termodinamika Organicheskikh Soedineniy (1986) 77–80.
[15] A.I. Gubareva, P.A. Gerasimov, V.V. Veregovykh, Zh. Prikl. Khim. 10 (1984) 2383–2385.
[16] A.V. Blokhin, Y.U. Paulechka, G.J. Kabo, J. Chem. Eng. Data 51 (2006) 1377–1388.
[17] H.J. Hoge, J. Res. NBS 36 (1946) 111–118.
[18] NIST ThermoData Engine Version 8.0 – Pure Compounds, Binary Mixtures, Reactions, NIST Standard Reference Database Number 103b, National Institute of Standards and Technology, Gaithersburg, MD.
[19] D.H. Zaitsau, S.P. Verevkin, A.Y. Sazonova, Fluid Phase Equilib. 386 (2015) 140–148.
[20] W. Wagner, A. Pruß, J. Phys. Chem. Ref. Data 31 (2002) 387–535.
[21] V.M. Sevruk, V.V. Simirsky, G.J. Kabo, A.A. Kozyro, A.P. Krasulin, Zh. Fiz. Khim. 64 (1990) 3402–3404.
[22] R. Sabbah, A. Xu-wu, J.S. Chickos, M.L.P. Leitão, M.V. Roux, L.A. Torres, Thermochim. Acta 331 (1999) 93–204.
[23] G.J. Kabo, A.V. Blokhin, A.G. Kabo, Chemical Problems of Creation of New Materials and Technologies, vol. 1, Belarusian State University (BSU), Minsk, 2003, pp. 176–193.
[24] A.B. Bazyleva, A.V. Blokhin, A.G. Kabo, G.J. Kabo, V.N. Emel'yanenko, S.P. Verevkin, J. Chem. Thermodyn. 40 (2008) 509–522.
[25] W.N. Hubbard, D.W. Scott, G. Waddington, in: F.D. Rossini (Ed.), Experimental Thermochemistry. Measurement of Heats of Reaction, Interscience Publishers, New York, 1956.
[26] D. Wagman, W.H. Evans, V.B. Parker, R.H. Schumm, I. Halow, S.M. Bailey, K.L. Churney, R.L. Nuttall, J. Phys. Chem. Ref. Data 11 (Suppl. 2) (1982) 392.
[27] M.E. Wieser, N. Holden, T.B. Coplen, J.K. Böhlke, M. Berglund, W.A. Brand, P.D. Bièvre, M. Gröning, R. De Loss, J. Meija, T. Hirata, T. Prohaska, R. Schoenberg, G. O'Connor, T. Walczyk, S. Yoneda, X.K. Zhu, Pure Appl. Chem. 85 (2013) 1047–1078.
[28] J.D. Cox, D.D. Wagman, V.A. Medvedev, CODATA Key Values for Thermodynamics, Hemisphere Pub. Corp, New York, 1989.
[29] A.D. Becke, J. Chem. Phys. 98 (1993) 5648–5652.
[30] C. Lee, W. Yang, R.G. Parr, Phys. Rev. B 37 (1988) 785–789.
[31] M.J. Frisch, G.W. Trucks, H.B. Schlegel, G.E. Scuseria, M.A. Robb, J.R. Cheeseman, G. Scalmani, V. Barone, B. Mennucci, G.A. Petersson, H. Nakatsuji, M. Caricato, X. Li, H.P. Hratchian, A.F. Izmaylov, J. Bloino, G. Zheng, J.L. Sonnenberg, M. Hada, M. Ehara, K. Toyota, R. Fukuda, J. Hasegawa, M. Ishida, T. Nakajima, Y. Honda, O. Kitao, H. Nakai, T. Vreven, J.A. Montgomery Jr., J.E. Peralta, F. Ogliaro, M.J. Bearpark, J. Heyd, E.N. Brothers, K.N. Kudin, V.N. Staroverov, R. Kobayashi, J. Normand, K. Raghavachari, A.P. Rendell, J.C. Burant, S.S. Iyengar, J. Tomasi, M. Cossi, N. Rega, N.J. Millam, M. Klene, J.E. Knox, J.B. Cross, V. Bakken, C. Adamo, J. Jaramillo, R. Gomperts, R.E. Stratmann, O. Yazyev, A.J. Austin, R. Cammi, C.

Pomelli, J.W. Ochterski, R.L. Martin, K. Morokuma, V.G. Zakrzewski, G.A. Voth, P. Salvador, J.J. Dannenberg, S. Dapprich, A.D. Daniels, Ö. Farkas, J.B. Foresman, J.V. Ortiz, J. Cioslowski, D.J. Fox, Gaussian 09, Revision C.01, Gaussian Inc, Wallingford, CT, USA, 2009.
[32] A.D. Becke, Phys. Rev. A 38 (1988) 3098–3100.
[33] F. Neese, WiRes Comput. Mol. Sci. 2 (2011) 73–78.
[34] H. Kruse, S. Grimme, J. Chem. Phys. 136 (2012) 154101–154116.
[35] S. Grimme, J. Antony, S. Ehrlich, H. Krieg, J. Chem. Phys. 132 (2010) 154104–154119.
[36] S. Grimme, S. Ehrlich, L. Goerigk, J. Comput. Chem. 32 (2011) 1456–1465.
[37] T.J. Lee, G.E. Scuseria, Achieving Chemical Accuracy with Coupled-Cluster Theory, in: S.R. Langhoff (Ed.), Quantum Mechanical Electronic Structure Calculations with Chemical Accuracy, Springer, Netherlands, 1995, p. 1. Imprint: Springer, Dordrecht, online resource (402 pages).
[38] C. Riplinger, F. Neese, J. Chem. Phys. 138 (2013) 034106–034118.
[39] S. Grimme, J. Chem. Phys. 118 (2003) 9095–9102.
[40] F. Weigend, M. Häser, Theor. Chem. Acc. 97 (1997) 331–340.
[41] F. Neese, E.F. Valeev, J. Chem. Theory Comput. 7 (2011) 33–43.
[42] A. Schäfer, H. Horn, R. Ahlrichs, J. Chem. Phys. 97 (1992) 2571–2577.
[43] F. Weigend, R. Ahlrichs, Phys. Chem. Chem. Phys. 7 (2005) 3297–3305.
[44] E.F. Valeev, LIBINT: A library for the evaluation of molecular integrals of many-body operators over Gaussian functions, Version 2.1.0 (beta), <https://github.com/evaleev/libint>.
[45] A. Hansen, C. Bannwarth, S. Grimme, P. Petrović, C. Werlé, J.-P. Djukic, ChemistryOpen 3 (2014) 177–189.
[46] L.A. Curtiss, P.C. Redfern, K. Raghavachari, J. Chem. Phys. 126 (2007) 084108–084112.
[47] J.C. van Miltenburg, H. Gabrielová, K. Růžička, J. Chem. Eng. Data 48 (2003) 1323–1331.
[48] M. Zábranský, V.J. Růžička, J. Phys. Chem. Ref. Data 33 (2004) 1071–1081.
[49] Z. Kolská, J. Kukal, M. Zábranský, V. Růžička, Ind. Eng. Chem. Res. 47 (2008) 2075–2085.
[50] M. Straka, K. Růžička, M. Fulem, Thermochim. Acta 587 (2014) 67–71.
[51] E.S. Domalski, E.D. Hearing, J. Phys. Chem. Ref. Data 25 (1996) 1–525.
[52] E.C.W. Clarke, D.N. Glew, Trans. Faraday Soc. 62 (1966) 539–547.
[53] V. Majer, V. Svoboda, J. Pick, Heats of Vaporisation of Fluids, Elsevier, Elsevier Science Pub. Co., Distribution for USA and Canada, Amsterdam, New York, NY, 1989.
[54] B.E. Poling, J.M. Prausnitz, J.P. O'Connell, The Properties of Gases and Liquids, fifth ed., McGraw-Hill, New York, 2001.
[55] C.L. Yaws, Thermophysical Properties of Chemicals and Hydrocarbons, William Andrew, Norwich, NY, 2008.
[56] N. Cohen, J. Phys. Chem. Ref. Data 25 (1996) 1411–1481.
[57] J.B. Pedley, R.D. Naylor, S.P. Kirby, J.B. Pedley, Thermochemical Data of Organic Compounds, second ed., Chapman & Hall, London, 1986.
[58] Z. Kolská, V. Růžička, R. Gani, Ind. Eng. Chem. Res. 44 (2005) 8436–8454.
[59] K.S. Pitzer, J. Chem. Phys. 14 (1946) 239–243.
[60] R.D. Johnson, NIST Computational Chemistry Comparison and Benchmark Database, NIST Standard Reference Database Number 101, NIST, 2013.
[61] D.H. Zaitsau, Y.U. Paulechka, A.V. Blokhin, A.V. Yermalayeu, A.G. Kabo, M.R. Ivanets, J. Chem. Eng. Data 54 (2009) 3026–3033.
[62] J.R. Durig, A. Ganguly, A.M. El Defrawy, C. Zheng, H.M. Badawi, W.A. Herrebout, B.J. van der Veken, G.A. Guirgis, T.K. Gounev, J. Mol. Struct. 922 (2009) 114–126.
[63] A. Miani, V. Hänninen, M. Horn, L. Halonen, Mol. Phys. 98 (2000) 1737–1748.
[64] M. Umer, K. Leonhard, J. Phys. Chem. A 117 (2013) 1569–1582.
[65] D.L. Theobald, Acta Crystallogr. A 61 (2005) 478–480.
[66] W. Weltner Jr., K.S. Pitzer, J. Am. Chem. Soc. 73 (1951) 2606–2610.
[67] T.R.R. McDonald, C.A. Beevers, Acta Cryst. 5 (1952) 654–659.
[68] U. Gaur, B. Wunderlich, J. Phys. Chem. Ref. Data 10 (1981) 119–152.
[69] K.G. Joback, R.C. Reid, Chem. Eng. Commun. 57 (1987) 233–243.
[70] P. Basařová, V. Svoboda, Fluid Phase Equilib. 105 (1995) 27–47.
[71] L. Constantinou, R. Gani, AIChE J. 40 (1994) 1697–1710.
[72] M. Ducros, J.F. Gruson, H. Sannier, Thermochim. Acta 36 (1980) 39–65.
[73] S.P. Verevkin, J. Chem. Eng. Data 47 (2002) 1071–1097.

JCT 15-317